Cell Reports, Volume *23*

Supplemental Information

A Cyfip2-Dependent Excitatory Interneuron Pathway Establishes the Innate Startle Threshold

Kurt C. Marsden, Roshan A. Jain, Marc A. Wolman, Fabio A. Echeverry, Jessica C. Nelson, Katharina E. Hayer, Ben Miltenberg, Alberto E. Pereda, and Michael Granato

Supplemental Figures and Figure Legends

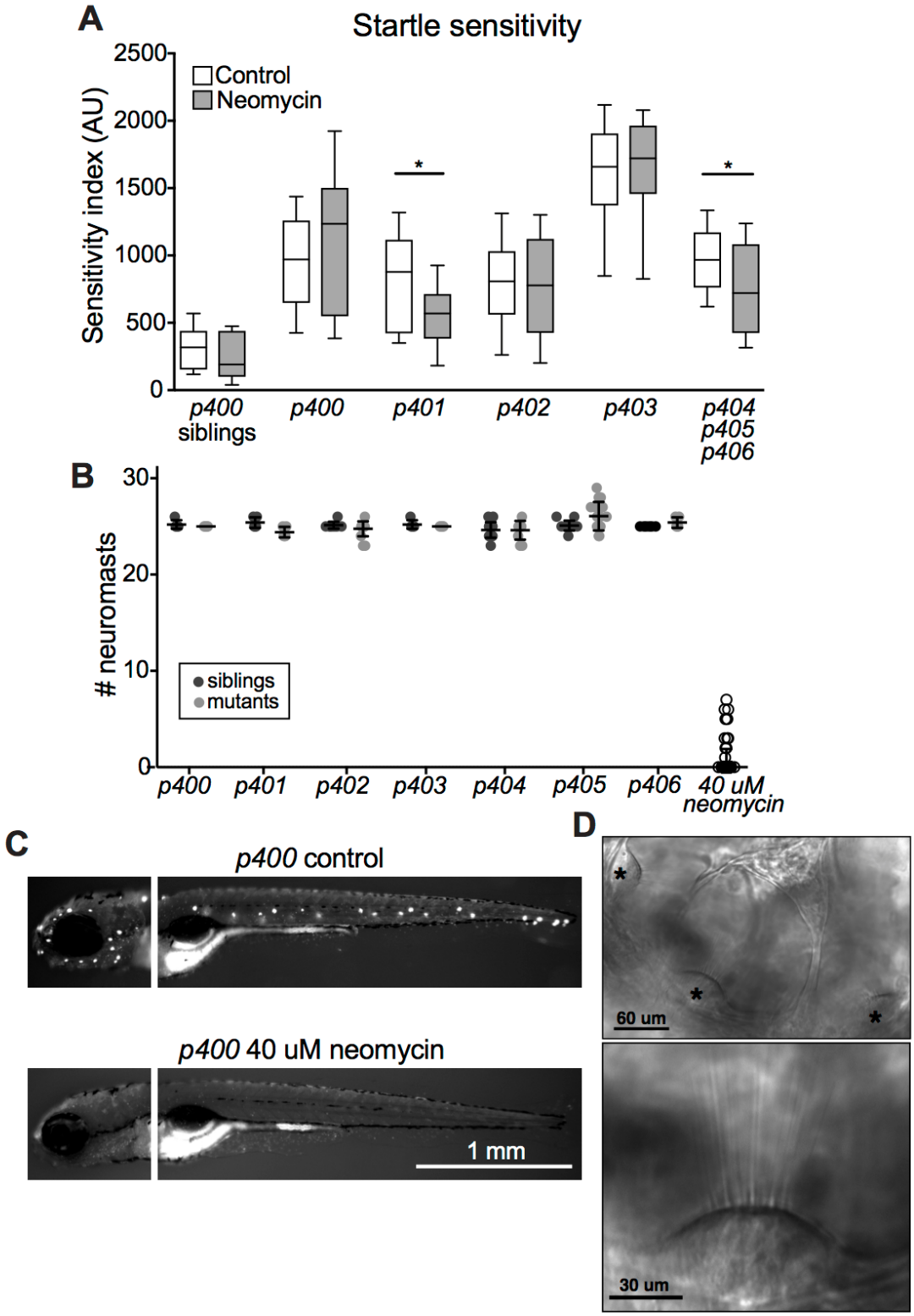

Figure S1. Otic vesicle and lateral line hair cell analysis, Related to Figure 1
(A) Boxplot showing startle sensitivity index after ablation of lateral line neuromasts with 40 μM neomycin. Sibling larvae are unaffected (n = 32 control, 27 neomycin), as are *p400* (n=22 con, 16 neo), *p402* (n=68 con, 68 neo), and *p403* (n=10 con, 9 neo) mutants. *p401* (n=22 con, 21 neo; *p=0.0320, Mann-Whitney) and *p404-6* (n=23 con, 40 neo; *p=0.0333, Mann-Whitney) mutants' sensitivity is partially rescued by lateral line ablation. (B)

Neuromast counts in siblings and mutants, based on DASPEI labeling. All larvae treated with 40 uM neomycin are grouped, with only a few individuals having intact neuromasts after treatment. (C) Images of DASPEI labeling of neuromasts in control and neomycin-treated *triggerhappy*^{p400} mutants. (D) Top, representative DIC images of otic vesicle showing the positions of the anterior, medial, and posterior hair cell bundles (asterisks). Bottom, magnification showing intact hair cell stereocilia. All mutants and siblings displayed similar morphology.

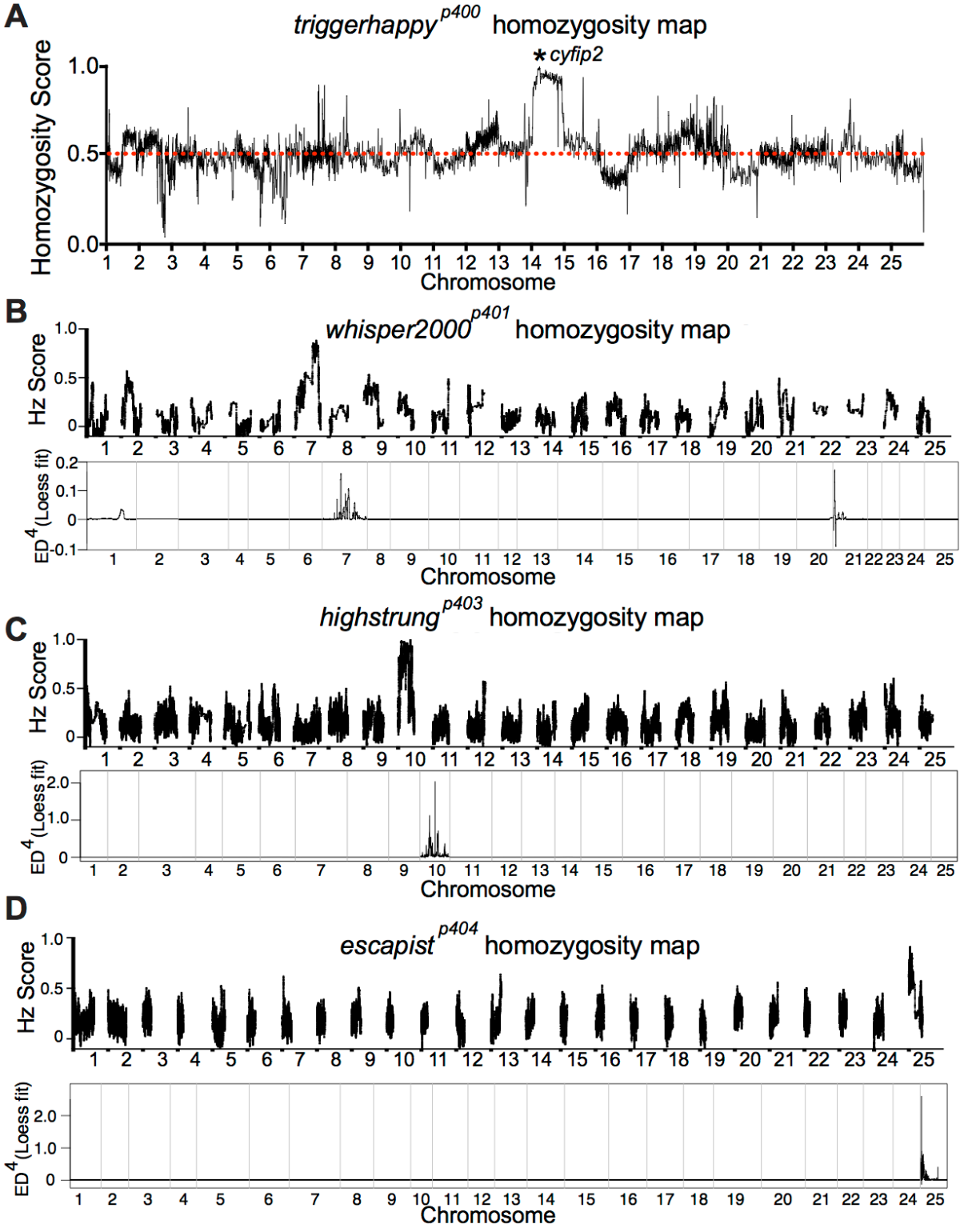

Figure S2. Homozygosity analysis links mutations to independent chromosomes, Related to Figure 2

(A) Whole genome sequence analysis of *triggerhappy*^{p400} mutants. Homozygosity scores close to 1.0 indicate linkage to TLF alleles; close to 0.0 indicates linkage to WIK alleles. Asterisk indicates the position of the identified nonsense mutation in *cyfip2* on chromosome 14. (B-D) Homozygosity analysis of RNAseq data in *whisper2000*^{p401}, *highstrung*^{p403}, and *escapist*^{p404} mutants. Top panels show the homozygosity plots using our customized analysis platform, with HZ scores of 1.0 indicating high homozygosity; bottom panels show the homozygosity analysis from MMAPPR analysis (Hill et al, 2013). Both methods agreed on linkage for each mutant. Furthermore, homozygosity analysis for all three *escapist* alleles (*p404-406*) revealed that all are linked to the same region of chromosome 25, supporting our complementation experiments.

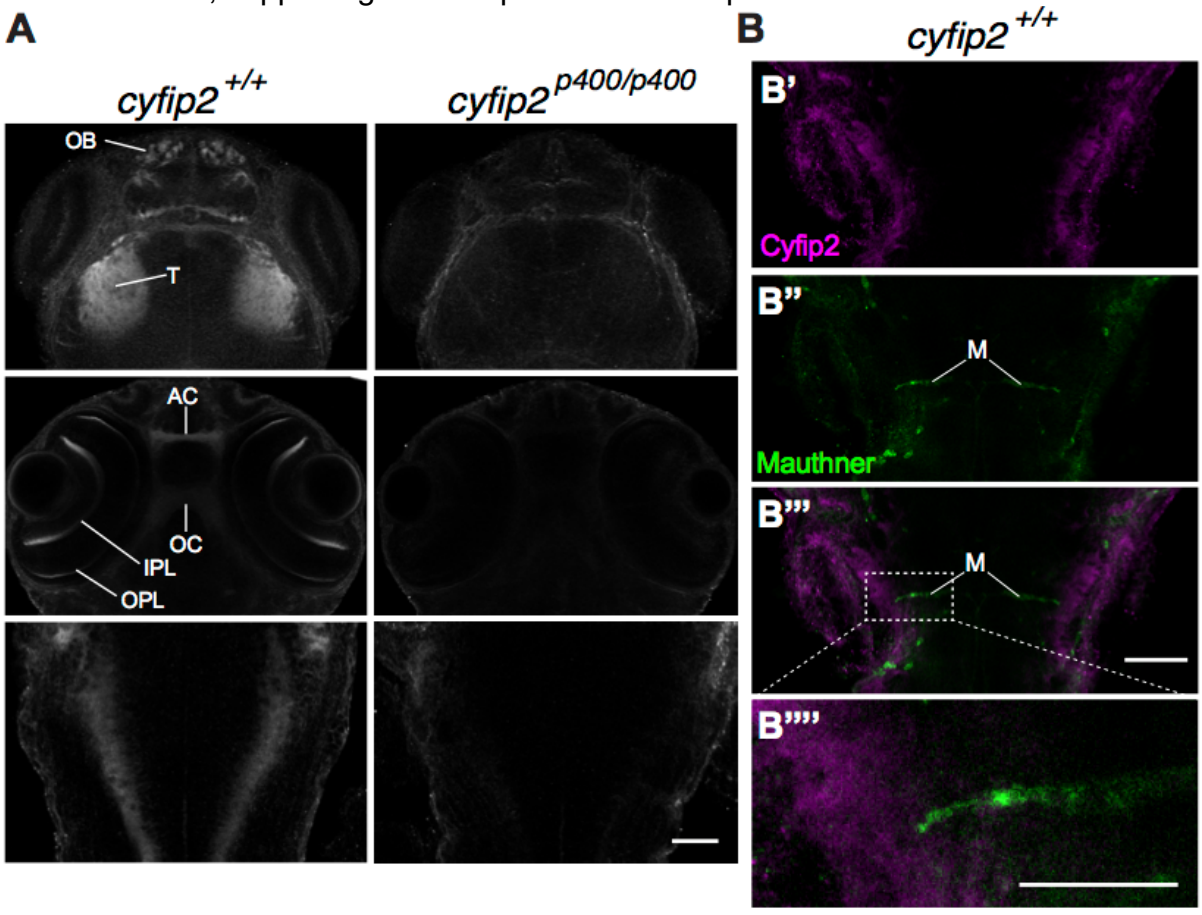

Figure S3. Cyfip2 is expressed broadly in neuropil; *Tg(hsp70:cyfip2-GFP)* is detectable in CNS for approximately 24 hours after heat shock, Related to Figure 2

(A) Cyfip2 Ab stain in *cyfip2*$^{+/+}$ and *cyfip2*$^{p400/p400}$ larvae at 72 hpf. OB: olfactory bulb, T: tectum, AC: anterior commissure, OC: optic chiasm, IPL: inner plexiform layer, OPL: outer plexiform layer (scale bar 30 μm). (B) Cyfip2 Ab stain (magenta) at 72 hpf showing labeling near the lateral dendrite of the Mauthner cell (M, green), labeled by *Tg(GFFDMC130A);Tg(UAS:gap43-citrine)* (scale bar: B'-B''': 30 μm; B'''': 15 μm). (C) Expression of *Tg(hsp70:cyfip2-GFP)* after a single 40 min heat shock at 37°C in larvae with (bottom) and without (top) the transgene. Scale bars 100 μm.

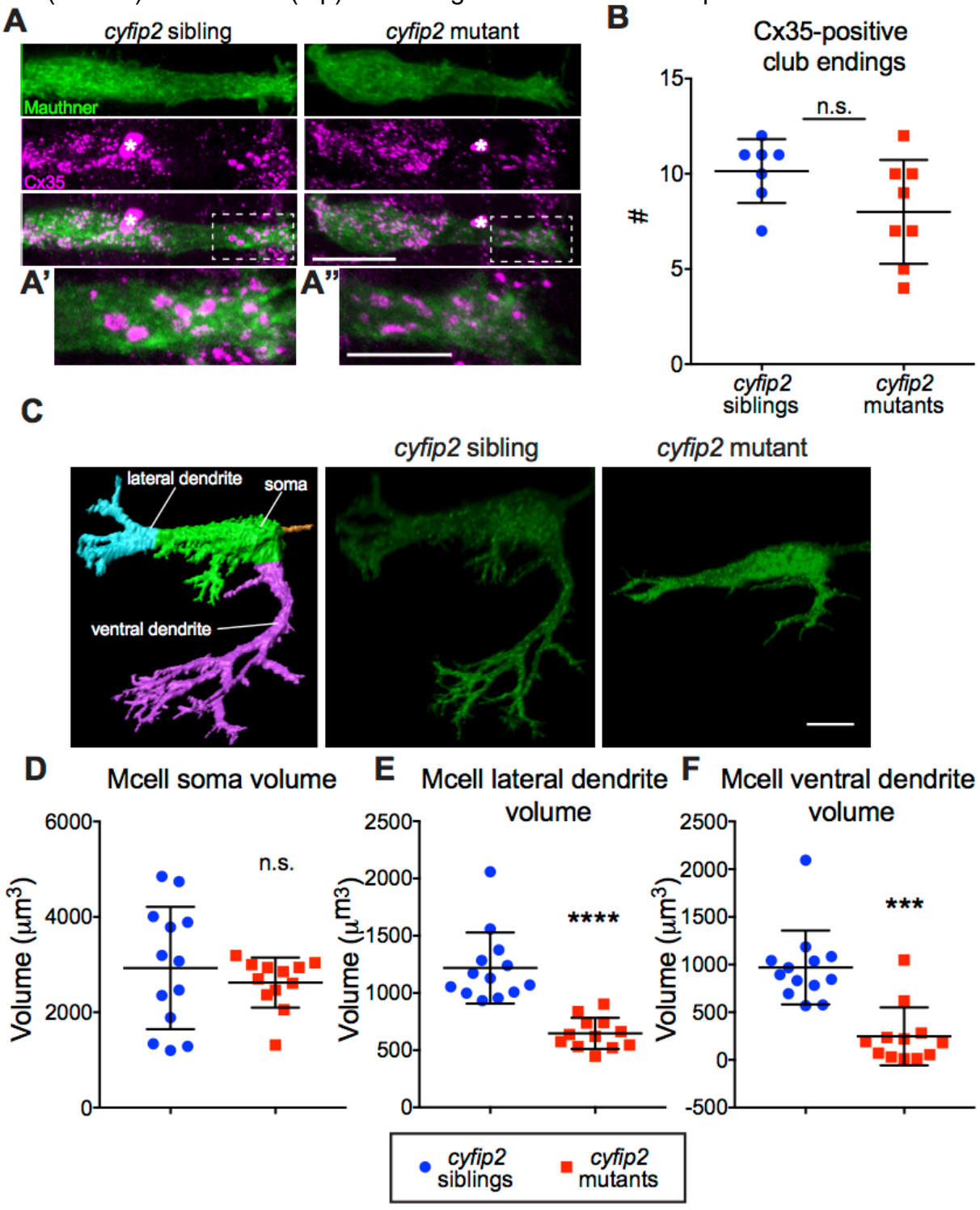

Figure S4. Mauthner cell club endings are normal but dendrite morphology is altered in *cyfip2* mutants, Related to Figure 3

(A) Images of Mcell gap junctions labeled by α-connexin 35 (Cx35) Ab (scale bar: 10 μm). Asterisks mark blood cells, dashed boxes highlight magnified region of lateral dendrite with club endings shown in (A') and (A") (scale bars: 5 μm). (B) Number of club endings (n=7 siblings, 8 mutants; p=0.11, Mann-Whitney; mean ± SD). (C) Confocal stacks of gap43-citrine-labeled Mcell membranes were masked and rendered in 3D using Imaris. Representative images show severely altered dendritic morphology in *cyfip2* mutants (scale bar: 5 μm). (D-E) Quantification of soma, lateral dendrite, and ventral dendrite volume (***p<0.001, ****p<0.0001; Mann-Whitney; mean ± SD).

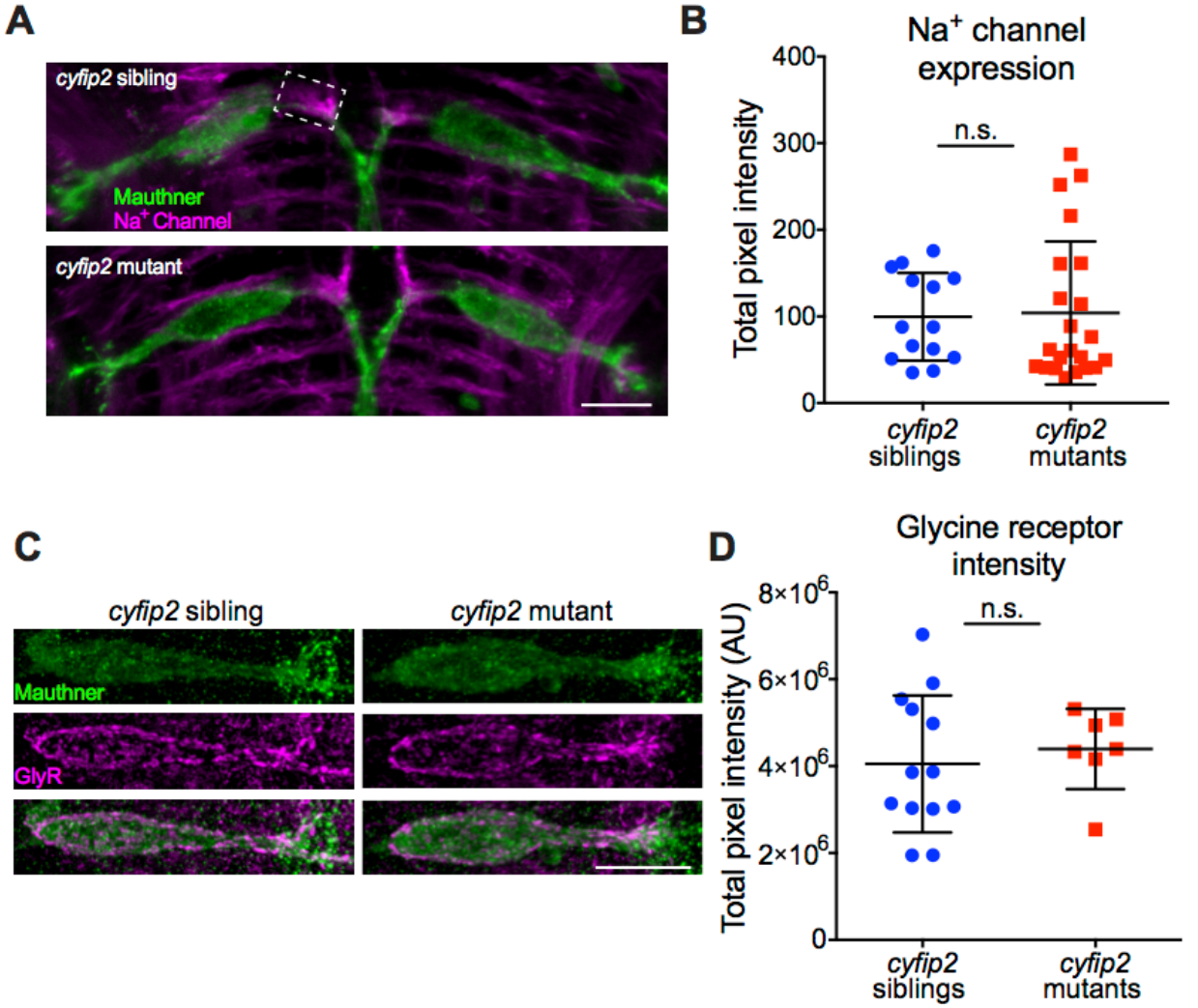

Figure S5. Sodium channel and Glycine receptor expression on the Mauthner cell is normal in *cyfip2* mutants, Related to Figure 3

(A) Representative images of maximum intensity projections of confocal stacks showing Mcell membranes (green), labeled by *Tg(GFFDMC130a);Tg(UAS:gap43-citrine)* and α-GFP Ab and sodium channels (Na^+ channel, magenta), labeled by a pan-Na^+ channel Ab (scale bar: 10 μm). Dashed box indicates the area of the Mcell axon cap that was analyzed in (B). (B) Quantification of Na^+ channel expression in the Mcell axon cap (n=14 siblings, 22 mutants; p=0.62, Mann-Whitney; mean ± SD). (C) Representative examples of *cyfip2* sibling and mutant Mcell glycine receptor (GlyR) expression. GlyR were labeled with an α-GlyR Ab (magenta) (scale bar: 10 μm). (D) Total intensity of GlyR staining on the Mcell was unchanged in *cyfip2* mutants (n=13 sibling larvae, 7 mutant larvae; p=0.59, Mann-Whitney; mean ± SD).

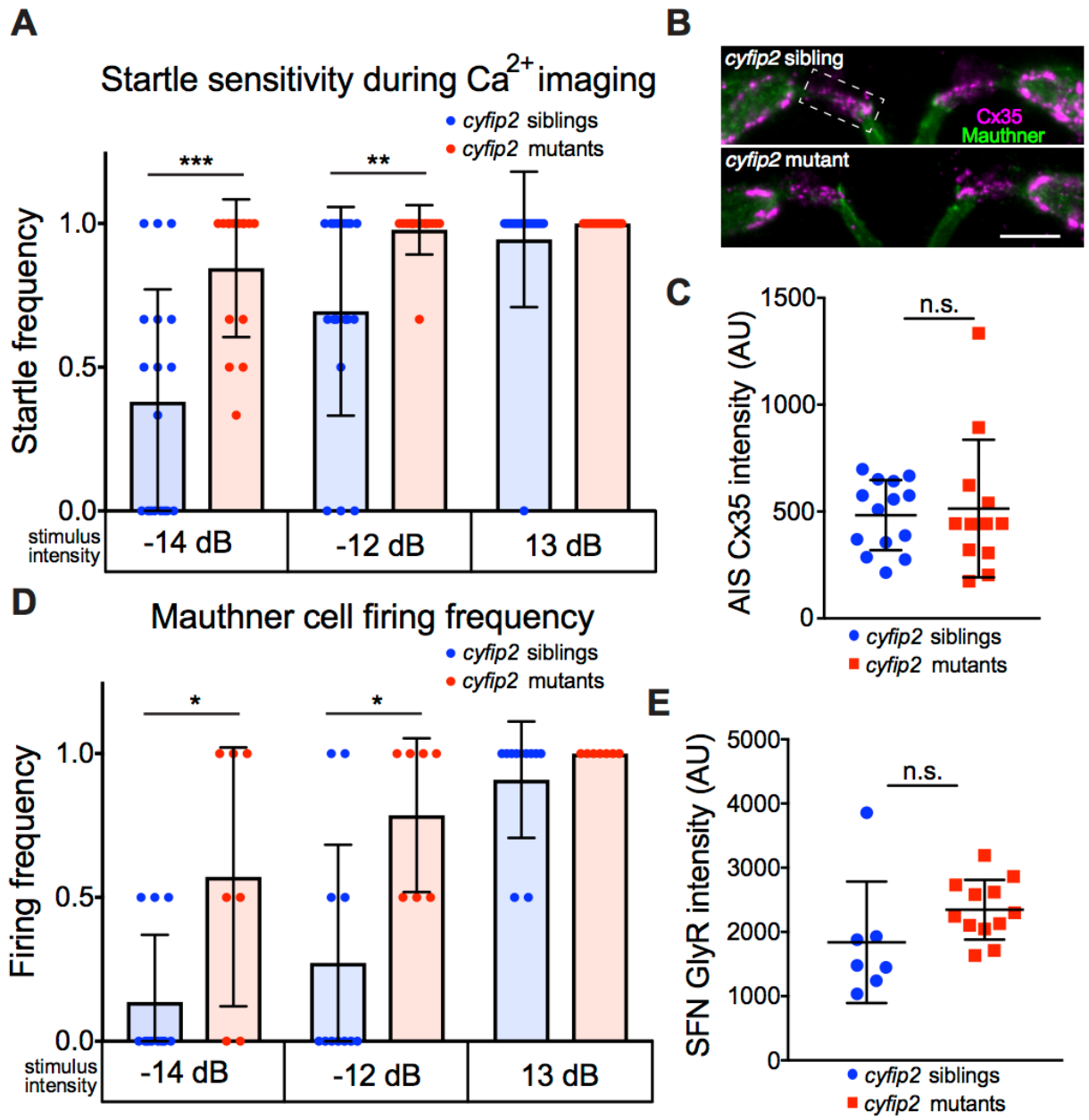

Figure S6. Startle sensitivity and Mauthner firing is increased in *cyfip2* mutants during *in vivo* Ca^{2+} imaging, Related to Figures 4 and 5

(A) Startle frequency in *cyfip2* siblings and mutants during head-restrained Ca^{2+} imaging following low (-14 dB), medium (-12 dB), and high (13 dB) intensity acoustic stimuli (**p<0.01, ***p<0.001, Mann-Whitney; mean ± SD). (B) Representative examples of Cx35 labeling of the Mcell axon initial segment (AIS). Dashed box indicates area analyzed in (C) (scale bar: 10 μm). (C) Quantification of Cx35 staining on Mcell AIS (n=14 siblings, 12 mutants; p=0.67; mean ± SD). (D) Mcell firing frequency in response to acoustic stimuli was measured by Ca^{2+} imaging in head-restrained 5 dpf larvae using *Tg(Gal4FF-62A);Tg(UAS:GCaMP6s)* (n=11 siblings, 7 mutants; *p<0.05, Mann-Whitney; mean ± SD). (E) Total intensity of GlyR staining on Spiral Fiber Neurons (SFN) was unchanged in *cyfip2* mutants (n=7 sibling larvae, 12 mutant larvae; p=0.13, Mann-Whitney; mean ± SD).

Table S1. PCR primers for molecular cloning and genotyping of *cyfip2*^{p400} and *cyfip2*^{tr230b}, Related to Figure 2

Primer	Forward	Reverse
genotyping		
fmr1^{hu2787} KASP	Proprietary	Proprietary
cyfip2^{p400} KASP	Proprietary	Proprietary
cyfip2^{p400} dCAPS	CAAAGTCTTGCTGCGGATAAAAG	CTGCACCATCTGCTCACACAAATT
cyfip2^{tr230b} dCAPS	TTGGGTGAATTCCATTTTTCA	CTCCAGGTGTACAACATGACAGC
GFP	GACGTAAACGGCCACAAGTT	GAACTCCAGCAGGACCATGT
cloning		
cyfip2 infusion	GATTCGAATTCAAGGCACCATGACAACCCACGTGACCCTGG	AGCACCTCCACCTCCACATGTGGTGGCCAGAGACTG
GFP infusion	GGAGGTGGAGGTGCTGTGAGCAAGGGCGAGGAGCTG	TAGAGGCTCGAGAGGTTACTTGTACAGCTCGTCCATGC
cDNA amplification		
cyfip2^{p400} SNP	CACCATCTGCTCACACAGG	CCCTGGCTTTCTATCACAGC

Table S2. Resources Table

REAGENT or RESOURCE	SOURCE	IDENTIFIER
Antibodies		
Rabbit anti-GFP	Life Technologies	Cat#A11122
Chicken anti-GFP	Aves Labs	Cat#GFP-120
Alexa488 Goat anti-Rabbit, highly cross-adsorbed	Life Technologies	Cat#A11034
Alexa488 Goat anti-Chicken, highly cross-adsorbed	Life Technologies	Cat#A11039
Mouse anti-Cx35/36	Millipore	Cat#MAB3045
Alexa594 Goat anti-Mouse IgG, highly cross-adsorbed	Life Technologies	Cat#A11032
Mouse anti-GlyR	Synaptic Systems	Cat#146011
Mouse pan anti-Sodium channel	Sigma	Cat#S8809
Rabbit anti-Cyfip2	Abcam	Cat#ab95969
Chemicals, Peptides, and Recombinant Proteins		
Rhodamine-dextran MW 10000	Life Technologies	Cat#D1824
Neomycin	Sigma	Cat#N1142
DASPEI	Invitrogen	Cat#D426
(+)-Tubocurarine Chloride	Millipore	Cat#505145
Experimental Models: Organisms/Strains		
Zebrafish: (Tüpfel Long Fin, TLF) wild type	(Wolman et al., 2015)	ZFIN: ZDB-GENO-151014-6
Zebrafish: (WIK-L11) wild type	(Wolman et al., 2015)	ZFIN: ZDB-GENO-010531-2
Zebrafish: *Tg(hsp70:GAL4FFDMC)130a; Tg(UAS:gap43-citrine)*	(Pujol-Marti et al., 2012); (Lakhina et al., 2012)	ZFIN: ZDB-ALT-120320-6; ZDB-FISH-150901-21649

Zebrafish: *Tg(hsp70GFF62A); Tg(UAS:gcamp6s)*	(Yamanaka et al., 2013); (Marsden and Granato, 2015)	ZFIN: ZDB-ALT-150717-1; ZDB-TGCONSTRCT-160316-3
Zebrafish: *Tg(-6.7Tru.Hcrt:GAL4-VP16); Tg(14xUAS:GCaMP5)*	(Lacoste et al., 2015)	ZDB-ALT-151028-4
Zebrafish: *Tg(SCP1:Gal4FF(y256Et))*	(Marquart et al., 2015)	ZDB-ALT-151216-14
Zebrafish: *Et(T2KHG)zf206, Tol056*	(Satou et al., 2009)	ZDB-ALT-110217-6
Zebrafish: *fmr1*^{hu2787}	(Broeder et al., 2009)	ZDB-ALT-090611-7
Zebrafish: *nevermind/cyfip2*^{tr230b}	(Trowe et al., 1996); (Pittman et al., 2010)	ZDB-ALT-980203-1245
Zebrafish: *triggerhappy/cyfip2*^{p400}	This paper	ZDB-ALT-180305-9
Zebrafish: *whisper2000*^{p401}	This paper	ZDB-ALT-180305-10
Zebrafish: *detector*^{p402}	This paper	ZDB-ALT-180305-11
Zebrafish: *highstrung*^{p403}	This paper	ZDB-ALT-180305-12
Zebrafish: *escapist*^{p404}	This paper	ZDB-ALT-180305-13
Zebrafish: *escapist*^{p405}	This paper	ZDB-ALT-180305-14
Zebrafish: *escapist*^{p406}	This paper	ZDB-ALT-180305-15
Zebrafish: *Tg(hsp70:cyfip2-EGFP)*	This paper	ZDB-ALT-180309-1
Oligonucleotides		
Primers for amplifying and genotyping GFP and *fmr1* and *cyfip2* mutations, see Table S1		
Recombinant DNA		
pCR4 cyfip2 plasmid	Thermofisher	CloneId: 9038384
pENTR cyfip2-GFP plasmid	This paper	N/A
pDEST hsp70: cyfip2-GFP plasmid	This paper	N/A
pCR2.1 cyfip2 cDNA	This paper	N/A
Software and Algorithms		
FLOTE & DAQTimer	(Burgess and Granato, 2007)	https://science.nichd.nih.gov/confluence/display/burgess/Software
Imaris	Bitplane	http://www.bitplane.com/download
GraphPad Prism	GraphPad Software	https://www.graphpad.com/
dCAPS	(Neff et al., 2002)	http://helix.wustl.edu/dcaps/dcaps.html
ImageJ	NIH	https://imagej.net/Fiji/Downloads

Supplemental Experimental Procedures

Zebrafish husbandry and maintenance

Embryos were raised at 29ºC on a 14-h:10-h light:dark cycle in E3 media as described previously (Burgess and Granato, 2007). *nevermind* (*cyfip2*^{tr230b}) carriers were provided

by John Gaynes (Pittman et al., 2010). *Tg(-6.7FRhcrtR:gal4VP16); Tg(UAS:GCaMP5)* fish were provided by David Schoppik (Lacoste et al., 2015), and *Tg(SCP1:Gal4FF(y256Et)* fish were provided by Harry Burgess (Marquart et al., 2015). *Tg(GFFDMC130A)* and *Tg(GFF62A)* were provided by Koichi Kawakami (Pujol-Martí et al., 2012; Yamanaka et al., 2013). *Tg(UAS:gap43-citrine)* fish were provided by Jonathan Raper (Lakhina et al., 2012).

Generation of* hsp70:cyfip2-GFP *transgenic line and genotyping

To create the *Tg(hsp70:cyfip2-GFP)* line a pCR4-cyfip2 plasmid containing the zebrafish *cyfip2* cDNA was purchased from ThermoFisher (CloneId:9038384), with the complete correct sequence confirmed by PCR amplification and Sanger sequencing. Infusion cloning (Clontech) was used to ligate PCR-amplified *cyfip2* cDNA and GFP into a Gateway (Invitrogen) pENTR plasmid cut with EcoRI and XhoI. Gateway cloning using LRII+ enzyme (Invitrogen) moved *cyfip2*-GFP to a pDEST plasmid containing the hsp70 promoter and I-SceI restriction sites. I-SceI-mediated transgenesis was done in TLF embryos as described (Thermes et al., 2002). Transgenic lines were identified by placing 24 hpf embryos produced by injected fish into eppendorf tubes at 37°C for 30 min, recovering in petri dishes for 60 min, and screening for GFP with a fluorescent stereomicroscope (Olympus MVX10). 3 lines were identified, and the one used in this study was chosen on the basis of its CNS-restricted pattern of expression (Fig. S2C).

cyfip2^{p400} and *fmr1*^{hu2787} fish were genotyped using the KASP method with proprietary primer sequences (LGC Genomics). For genotyping in the context of *Tg(hsp70:cyfip2-GFP)* we developed a dCAPS assay using the dCAPS program (http://helix.wustl.edu/dcaps/dcaps.html) to design appropriate primers, with the forward primer binding in the intron adjacent to the mutation (Table S1) (Neff et al., 2002).

Following gDNA isolation, a 149 bp fragment was amplified by PCR and the product was digested with ApoI-HF (New England Biolabs), cleaving the mutant allele and producing a 125 bp fragment distinguishable from the 149 bp wild type allele on a 3% agarose gel containing 1.5% Metaphor agarose (Lonza). Genotyping for the presence of the *Tg(hsp70:cyfip2-GFP)* transgene was done with primers specific to GFP (Table S1). *cyfip2*^{tr230b} fish were genotyped by dCAPS as described (Pittman et al., 2010); Table S1).

Behavioral assays and analysis

Behavioral experiments were performed using 4-6 dpf larvae and analyzed using FLOTE software as described previously (Burgess and Granato, 2007; Hao et al., 2013; Wolman et al., 2011; 2015). Startles (short-latency C-bends) were measured using defined kinematic parameters (latency, turn angle, duration and maximum angular velocity). Startle sensitivity was determined by measuring startle frequency using a 60-stimulus assay with 20 s ISI and 10 trials at each of the following intensities: 4.6 dB, 13.5 dB, 17.2 dB, 20.7 dB, 23.9 dB, 25.9 dB. Sensitivity index was calculated for each larva by measuring the area under the curve of startle frequency v. stimulus intensity using Prism software (GraphPad). For secondary behavioral analysis (baseline activity, startle habituation, PPI, neomycin sensitivity) mutants and siblings were first identified using a 20-stimulus assay consisting of 10 stimuli at 13.5 dB and 10 stimuli at 17.2 dB with 20 s ISI. Mutants were defined as those responding to >50% of stimuli at both intensities; siblings were defined as those responding between 10-20% across all stimuli. Total distance traveled over 160s was measured to determine baseline activity. Startle habituation (Wolman et al., 2011; 2015) and PPI (Burgess and Granato, 2007) were measured as described, using a 13.5 dB pre-pulse and 25.9 dB pulse with 350 msec ISI. The PPI hearing threshold (Bhandiwad et al., 2013) was determined using 6 intensities

of pre-pulse (-14.9, -1.1, 4.6, 10.2, 13.5, and 17.2 dB), with pairs of stimuli separated by 20s. Significant PPI was defined by comparing startle frequency in pre-pulse trials to pulse only trials ($p<0.05$, paired t-test). All stimuli were calibrated with a PCB Piezotronics accelerometer (#355B04) and signal conditioner (#482A21), and voltage outputs were converted to dB using the formula dB = 20 log (V / 0.775).

Molecular cloning of* cyfip2 *and RNAseq analysis

To identify potential causative mutations in *triggerhappy*^{p400} we identified all SNPs in the linked region of chromosome 14 that were unique to *triggerhappy*^{p400} in comparison to a combined reference sequence consisting of the Ensembl zebrafish genome (Zv9), our TLF and WIK sequences, and our other mutant sequences (Wolman et al., 2015). Candidate mutations were defined as those SNPs with <1% allele frequency in this reference sequence and >95% allele frequency in the mutant sample that cause a change in the amino acid sequence (nonsense, missense, or splice site mutations). This produced a single SNP candidate for *triggerhappy*^{p400}. To confirm the candidate mutation in *cyfip2* we prepared cDNA from identified siblings and mutants as described (Wolman et al., 2015). Amplified *cyfip2* cDNA was cloned into a pCR2.1-TOPO-TA vector for sequencing.

Mapping of *whisper2000*^{p401}, *highstrung*^{p403}, and *escapist*$^{p404-6}$ was performed using RNAseq. F5 mutants and siblings of *whisper2000*^{p401}, *highstrung*^{p403}, and *escapist*$^{p404-6}$ were collected, and RNA was extracted. 125bp paired-end sequencing was conducted using the Illumina HiSeq 2000 platform, and homozygosity mapping was done by comparing mutant and sibling sequences using the MMAPPR pipeline as described (Hill et al., 2013). In parallel, we adapted our WGS pipeline to analyze RNAseq data by isolating an exomic set of SNPs unique to each mutant family. SNPs were defined as

chromosomal locations in the sibling pool in which exactly two bases account for greater than 90% of the obtained sequence reads at a given position, and each of these two alleles is observed in greater than 25% of reads. Homozygosity in the mutant pool was calculated for each of these SNP positions. To identify linked regions of the genome we then plotted the difference between mutant and sibling homozygosity, with scores close to 1 indicating strong linkage.

Immunohistochemistry, spinal backfills, DASPEI staining, and image analysis

Primary antibodies used were: chicken anti-GFP (Aves Labs, #GFP-120; 1:500), rabbit anti-GFP (Life Technologies, #A11122; 1:500), anti-Cx35/36 (Millipore, #MAB3045; 1:200), anti-GlyR (Synaptic Systems, #146011; 1:200), pan anti-Sodium channel (Sigma, #S8809; 1:500), anti-Cyfip2 (abcam, #ab95969; 1:100). Images were acquired using a Zeiss LSM-710 or 880 confocal microscope. For spinal backfill-labeling of reticulospinal neurons, 5 dpf larvae were anaesthetized in 0.2% tricaine (Sigma), and neurons were labeled using a glass pipette backfilled with rhodamine-dextran (Life Technologies, MW 3000; 5% in 0.2 M KCl) injected into the spinal cord at the level of the anus. DASPEI labeling and counting of lateral line neuromasts was done using a fluorescent macroscope (Olympus MVX10) as described (Harris et al., 2003). Otic vesicle hair cells were imaged using DIC optics on a Zeiss Axio Scope.

Confocal stacks were used to quantify M-cell morphology with Imaris software (Bitplane) by creating a M-cell surface based on the anti-GFP Ab-amplified *Tg(GFFDMC130A);Tg(UAS:gap43-citrine)* signal. The cell was segmented by creating a cut plane at the inflection point between the ventral dendrite and the soma to isolate the ventral dendrite, and to isolate the lateral dendrite a vertical cut plane was placed 30 μm from the distal-most extent of the lateral dendrite. The remaining central portion was

defined as the soma. Quantification of Cx35-labeled M-cell club endings was done with Imaris by first creating an M-cell surface based on the anti-GFP Ab-amplified *Tg(GFFDMC130A);Tg(UAS:gap43-citrine)* signal and masking the Cx35 signal with this surface. We then created surfaces from the masked Cx35 channel, and counted the number of surfaces on the lateral dendrite that had volumes greater than 750 voxels. Sodium channel and Cx35 labeling at the M-cell AIS was done by first isolating the M-cell surface, creating cut planes at the inflection point between the soma and AIS and at the crossing of the two M-cell axons, and masking the sodium channel or Cx35 channel. Total intensity above background within this volume was recorded. M-cell GlyR analysis was also done by creating a M-cell surface using the anti-GFP Ab-amplified *Tg(GFFDMC130A);Tg(UAS:gap43-citrine)* signal. The GlyR channel was masked with the M-cell surface, and the total pixel intensity above background was normalized to the volume of the surface. Spiral fiber (SF) GlyR expression was similarly analyzed in Imaris, using the anti-GFP Ab-amplified *Tg(-6.7FRhcrtR:gal4VP16);Tg(UAS:GCaMP5)* signal to create a surface encompassing the SF population, masking the GlyR channel with this surface, and normalizing the total pixel intensity to the SF neuron cluster volume. Staining, imaging, and analysis were all done blind to genotype, with genotyping after completing image analysis.

Combined Ca^{2+} and behavior imaging and analysis

5 dpf *Tg(-6.7FRhcrtR:gal4VP16); Tg(UAS:GCaMP5)* or *Tg(GFF62A);Tg(UAS:GCaMP6s)* larvae were semi-restrained in 2% agarose with tails freed distal to the swim bladder. GCaMP images were captured with a Leica DM16000 B inverted spinning disk confocal at 20 Hz and tail movements with a Dalsa Genie HM640 camera at 500 Hz. Analysis was done using Image J (NIH). ROIs were created manually for the SF axon terminals, SF

cell bodies, and M-cell soma. A background ROI was also created, and the mean pixel value of the background ROI was subtracted from the mean of each target ROI for all images in the sequence to calculate the intensity at each timepoint. F_0 was calculated by averaging the intensity of the 20 timepoints (1 s) immediately prior to the acoustic stimulus. Imaging and analysis was done blind to genotype, with genotyping after completion of the analysis.

Electrophysiology

Electrophysiological recordings were performed in 5-6 dpf *cyfip2*^{p400} siblings and mutants carrying the Tol056-GFP transgene that labels M-cells (Satou et al., 2009). For this purpose, larvae were paralyzed with d-tubocurarine (10 µM, Sigma) dissolved in external solution which consisted of (in mM): 134 NaCl, 2.9 KCl, 2.1 $CaCl_2$, 1.2 $MgCl_2$, 10 HEPES, 10 Glucose, pH 7.8 adjusted with NaOH (Koyama et al., 2011). The larvae were then placed on their backs and held with pins in a Sylgard-coated petri dish. The brain was ventrally exposed following the procedure described in (Koyama et al., 2011). Once dissected, larvae were transferred onto the recording setup and superfused with external solution. M-cells were identified using far-red DIC optics and GFP fluorescence. The patch pipette (4 MΩ) was filled with the following internal solution (in mM): 105 K-Methanesulfonate, 10 HEPES, 0.1 EGTA, 2 $MgCl_2$, 4 Na_2ATP, 0.4 Tris-GTP, 10 K_2-Phosphocreatine, 23 mannitol, pH 7.2 adjusted with KOH (Koyama et al., 2011). The estimated liquid junction potential was -16 mV. Current-clamp recordings were performed under the whole-cell configuration. The following parameters were estimated: 1) rheobase was determined by the minimum amount of positive current (10 ms in duration) needed to elicit an action potential, 2) voltage threshold was determined as the membrane potential at which a 10 ms depolarizing-current step elicits an action potential, 3) input

resistance was determined using the voltage deflection caused by a 1 nA hyperpolarizing-current step of 10 ms duration followed by the derivation of resistance using Ohm's law. To activate the auditory afferents terminating as club endings on the lateral dendrite of the M-cell, a "theta" (septated) glass pipette containing external solution was used as bipolar electrode and placed at the base of the posterior macula of the ear, near where dendritic processes of auditory afferents contact the hair cells and where the large somata of these afferents are located (Fig. 3A). The amplitude of the electrical and chemical components of the mixed synaptic potentials was measured at the maximum synaptic response, at which all club ending afferents are stimulated. Maximum response was set by gradually increasing stimulus intensity while monitoring the amplitude of the electrical component of the mixed response until its maximum amplitude was reached and where further increase in stimulus strength would recruit other, delayed, synaptic potentials originated by stimulation of fibers with slower conduction velocities (Yao et al., 2014). The paired-pulse ratio (PPR) was calculated as the ratio between the amplitude of the second and the first chemical component of the mixed synaptic response (second chemical/first chemical) in response to paired stimuli with a 2 ms interval. Traces representing the average of at least 10 individual responses were used for measurements of synaptic potentials. After recording, larvae were frozen in methanol, and DNA extracted and genotyped.

Supplemental References

Hao, L.T., Duy, P.Q., Jontes, J.D., Wolman, M., Granato, M., and Beattie, C.E. (2013). Temporal requirement for SMN in motoneuron development. Hum. Mol. Genet. *22*, 2612–2625.

Lakhina, V., Marcaccio, C.L., Shao, X., Lush, M.E., Jain, R.A., Fujimoto, E., Bonkowsky, J.L., Granato, M., and Raper, J.A. (2012). Netrin/DCC signaling guides olfactory sensory axons to their correct location in the olfactory bulb. J. Neurosci. *32*, 4440–4456.

Neff, M.M., Turk, E., and Kalishman, M. (2002). Web-based primer design for single nucleotide polymorphism analysis. Trends Genet. *18*, 613–615.

Pujol-Martí, J., Zecca, A., Baudoin, J.-P., Faucherre, A., Asakawa, K., Kawakami, K., and López-Schier, H. (2012). Neuronal birth order identifies a dimorphic sensorineural map. J. Neurosci. *32*, 2976–2987.

Thermes, V., Grabher, C., Ristoratore, F., Bourrat, F., Choulika, A., Wittbrodt, J., and Joly, J.-S. (2002). I-SceI meganuclease mediates highly efficient transgenesis in fish. Mech. Dev. *118*, 91–98.

Yamanaka, I., Miki, M., Asakawa, K., Kawakami, K., Oda, Y., and Hirata, H. (2013). Glycinergic transmission and postsynaptic activation of CaMKII are required for glycine receptor clustering in vivo. Genes Cells *18*, 211–224.